PHYSICAL REVIEW D VOLUME 39, NUMBER 4 15 FEBRUARY 1989

Formation of a "child" universe in an inflationary cosmological model

Katherine A. Holcomb
Computation Center, University of Texas, Austin, Texas 78712

Seok Jae Park and Ethan T. Vishniac
Department of Astronomy, University of Texas, Austin, Texas 78712
(Received 26 August 1988)

The evolution of a flat, spherically symmetric cosmological model, containing radiation and an inhomogeneous scalar field, is simulated numerically to determine whether the inhomogeneity could cause a "child" universe, connected by a wormhole to the external universe, to form. The gravitational and field quantities were computed self-consistently by means of the techniques of numerical relativity. Although we were unable to follow the process to its completion, preliminary indications are that the "budding" phenomenon could occur under very general initial conditions, as long as the scalar field is sufficiently inhomogeneous that the wormhole forms before the inflation is damped by the expansion of the background spacetime.

I. INTRODUCTION

Observations of the microwave background provide strong evidence for the large-scale homogeneity and isotropy of the present Universe. Other observations indicate that the dynamical value for Ω, the ratio of actual to critical energy density, is in the range $0.1 \lesssim \Omega \lesssim 0.3$. Unfortunately, the isotropy and homogeneity of the Universe, and the surprising nearness of Ω to the magic value of unity, are difficult to explain in the context of the "standard model" of the evolution of the Universe without severe constraints on the initial conditions. The inflationary scenario[1-3] offers the promise of accounting for these phenomena in a natural way.

The inflationary model requires that at some very early epoch in the history of the Universe, the energy density was dominated by the potential energy associated with a scalar field φ. Provided the field evolves sufficiently slowly, the major contribution to the energy density for many expansion times would be the potential $V(\varphi)$. In this case the Universe would expand exponentially rather than according to a power law. This "inflationary" period, during which the volume of the Universe expands by many orders of magnitude, ensures that locations on the sky that are widely separated today were in causal contact before the beginning of inflation, thus explaining the observed high degree of isotropy in the microwave background.

Unfortunately, this simple scenario actually begs the question which we wish it to answer; although the inflationary model is invoked to explain the isotropy and homogeneity of the Universe, for the currently accepted behavior of the potential, inflation is inevitable only in spacetimes that are already homogeneous and isotropic. In general, the requirement that $V(\varphi)$ dominate the energy density is only occasionally satisfied. Random fluctuations in the amplitude of the field, the contributions to the energy density of other components of the primordial plasma, and the structure of spacetime itself, will usually prevent inflation from occurring. The general case is thus one in which a "chaotic" spacetime evolves small patches which inflate.[4]

It has been suggested[5] that this process could produce closed second-generation universes which would be connected to the "mother" universe through a wormhole. Analytic calculations of an idealized system, a spherical region of false vacuum separated by an infinitesimally thin domain wall from a region of true vacuum, have been carried out by many workers.[6] While their results are significant and serve to illuminate the process by which "budding" of universes could occur,[7] the process should be studied with a more realistic structure for the scalar field. Since analytic solutions are currently impossible for general inhomogeneous cosmologies, such an investigation will almost certainly necessitate a numerical approach. Kurki-Suonio, Centrella, Matzner, and Wilson[8] have studied numerically the behavior of an inhomogeneous scalar field, but they did not attempt to follow the interface between the true and false vacua, as they wished to determine only whether such a scalar field would allow a global inflation to occur at all. If a "child" universe is to be created, however, a small portion of the Universe inflates while the rest continues to evolve as an Einstein–de Sitter spacetime. An observer external to the inflating region sees what appears to him to be the formation of a black hole, which cuts off the communication between the "child" universe and the external universe. Inside the "bud," the total energy due to the matter, excluding gravitational contributions, can greatly exceed the energy of the wormhole. This region of spacetime continues to evolve independently even though the black hole rapidly evaporates; thus the wormhole effectively creates a new universe, which by its inflation could grow to account for our entire observable Universe.

It is this phenomenon which we wish to study; this paper is a report of the results of the numerical study of the evolution of a spacetime containing a simplified but nontrivial inhomogeneous scalar field. The gravitational variables must be evolved along with the matter variables for a consistent treatment, which requires the application of the techniques of numerical relativity.

II. FORMALISM

The traditional approach to numerical relativity is the Arnowitt-Deser-Misner[9] (ADM) "3+1" formalism, in which spacetime is broken down into spacelike hypersurfaces, each of which is a level surface of the congruence of timelike curves that specifies the time coordinate. The general (ADM) metric can be written in the form

$$ds^2=-(\alpha^2-\beta_i\beta^i)dt^2+2\beta_i dx^i dt + \gamma_{ij}dx^i dx^j , \tag{1}$$

where α, the *lapse function,* and $\boldsymbol{\beta}$, the shift vector, accommodate the 4 degrees of freedom due to general covariance.

We use one of our degrees of freedom to specify the method by which the time-slice hypersurfaces are to be determined. To do so, it is sufficient to fix the trace of the extrinsic-curvature tensor, $K\equiv K^i_i$; this determines the lapse function and hence the time slicing. For cosmology, a natural choice is

$$K, \partial_t K = \text{functions of } t \text{ only} , \tag{2}$$

a criterion known as constant-mean-curvature slicing.

The remaining degrees of freedom determine the gauge conditions on the spatial coordinates. In analytic work the condition $\boldsymbol{\beta}=0$ is generally used; when taken in conjunction with the requirement that $\alpha=1$, the result is known as geodesic slicing or Gaussian normal coordinates. Unfortunately, such coordinates have proven unsuitable for numerical work, as they tend to result in coordinate singularities in strong-field situations.[10] We shall instead employ our gauge freedom to force the spatial metric to be as simple as possible.[11] In the case of spherical symmetry, this leads to a radial coordinate which is isotropic, and the final form for the metric is

$$ds^2=-(\alpha^2-\beta^2)dt^2+2\beta\, dr\, dt + A^2(dr^2+r^2 d\theta^2+r^2\sin^2\theta\, d\phi^2) , \tag{3}$$

where $\beta\equiv\beta^r$ is the only nonzero component of the shift vector.

We must now specify a stress-energy tensor for our spacetime. We shall assume the matter in our cosmology consists of two *noninteracting* substances, a relativistic perfect fluid, which models the radiation content of the early Universe, and a scalar field. Thus we may write

$$T_{\mu\nu}=T^{\text{fluid}}_{\mu\nu}+T^{\text{field}}_{\mu\nu} . \tag{4}$$

We choose units in which $G=c=\hbar=1$; in these units, the stress-energy tensor of the fluid is well known to be[12]

$$T^{\text{fluid}}_{\mu\nu}=\rho h u_\mu u_\nu + P g_{\mu\nu} , \tag{5}$$

where ρ is the rest-energy density of the fluid, u^μ is its four-velocity, and h is the specific relativistic enthalpy, defined to be

$$h=1+\epsilon+P/\rho . \tag{6}$$

The internal energy density of the fluid is defined to be $\rho\epsilon$, so ϵ is the specific energy density. In the case of radiation, for which $\rho=0$, ϵ alone will have no meaning, but it will always occur in combination with ρ in our equations.

If we assume the scalar field is a Higgs field, its stress-energy tensor is given by

$$T^{\text{field}}_{\mu\nu}=\partial_\mu\varphi\partial_\nu\varphi-[\tfrac{1}{2}\partial_\lambda\varphi\partial^\lambda\varphi+V(\varphi)]g_{\mu\nu} , \tag{7}$$

and we shall assume $V(\varphi)$ is of the Coleman-Weinberg[13] (CW) form

$$V(\varphi)=\lambda\varphi^4[\ln(\varphi^2/\sigma^2)-\tfrac{1}{2}]+\tfrac{1}{2}\lambda\sigma^4 . \tag{8}$$

We must now carry out the 3+1 split of the Einstein equations, inserting the above forms for the stress-energy tensor, to obtain the gravitational equations. By means of the Gauss-Codazzi equations, we obtain the constraint equations; the gravitational evolution equations are derived from the definition of the extrinsic-curvature tensor and the gauge conditions.[14,15] The results are displayed below.

Before we write out our equations, it is convenient to define

$$U\equiv\alpha u^0 , \tag{9a}$$

$$D\equiv\rho U , \tag{9b}$$

$$E\equiv\rho\epsilon U , \tag{9c}$$

$$v^r\equiv u^r/u^0 , \tag{9d}$$

and

$$K^*\equiv K^r_r-\tfrac{1}{3}K , \tag{9e}$$

$$\psi\equiv A^{1/2} , \tag{9f}$$

where $u^\mu=(u^0,u^r,0,0)$ is the four-velocity of the fluid.

One of the constraint equations involves the total energy density and hence is known as the Hamiltonian constraint:

$$\frac{1}{r^2}\partial_r(r^2\partial_r\psi)=-\tfrac{1}{4}\psi^5\{8\pi(D+E+PU)U-8\pi P +4\pi[\alpha^{-2}(\partial_t\varphi-\beta\partial_r\varphi)^2 + A^{-2}(\partial_r\varphi)^2] +8\pi V(\varphi)+\tfrac{1}{4}(3K^{*2}-\tfrac{4}{3}K^2)\} . \tag{10}$$

Note that the quantity $(\frac{1}{2}\{[(\partial_t\varphi-\beta\partial_r\varphi)/\alpha]^2+(\partial_r\varphi/A)^2\}+V(\varphi))$ plays the role of the energy density of the field.

In the case of spherical symmetry, there is only one independent momentum constraint. This equation applies only on a specific time slice, and is effectively a first-order ordinary differential equation which can be analytically reduced to a quadrature:

$$K^*=\frac{8\pi}{A^3r^3}\int_0^r A^3r'^3\{S_{r'}-[\alpha^{-1}\partial_{r'}\varphi(\partial_t\varphi-\beta\partial_{r'}\varphi)]\}dr' . \tag{11}$$

The equation for the shift variable is given by

$$\beta=-\tfrac{1}{2}r\int_r^\infty\frac{\alpha K^*}{r'}dr' . \tag{12}$$

Like the momentum constraint, this is a simple quadrature on a given time slice.

The next equation is that which specifies the lapse function. It is obtained from the equation for the evolution of the independent component of the extrinsic curvature tensor (K_r^r), but we take the viewpoint that K and $\partial_t K$ are predetermined, and the lapse is computed from them:

$$\frac{1}{r^2}\partial_r[r^2\partial_r(\alpha\psi)]=\tfrac{1}{4}\alpha\psi^5\left[8\pi(D+E+PU)U\left[3-\frac{2}{U^2}\right]+40\pi P+28\pi\alpha^{-2}(\partial_t\varphi-\beta\partial_r\varphi)^2\right.$$
$$\left.-4\pi A^{-2}(\partial_r\varphi)^2-40\pi V(\varphi)+\tfrac{21}{4}K^{*2}+\tfrac{5}{3}K^2\right]+\psi^5(\beta\partial_r K-\partial_t K) . \tag{13}$$

An evolution equation can be written for the metric variable A; it takes the form of a "transport" equation:

$$\partial_t A^3-\frac{1}{r^2}\partial_r(r^2A^3\beta)=-\alpha K A^3 . \tag{14}$$

Now we lack only the matter equations. Since we assume that the field does not couple to the fluid, the equations of motion of the two kinds of matter can be derived independently. The fluid equations of motion are obtained from

$$T^{\mu(\text{fluid})}_{\nu;\mu}=0 \tag{15}$$

by means of appropriate projections with the fluid four-velocity.[16]

Particle-conservation equation:

$$\partial_t(DA^3)+\frac{1}{r^2}\partial_r(DA^3v^rr^2)=0 . \tag{16}$$

Energy equation:

$$\partial_t(EA^3)+\frac{1}{r^2}\partial_r(EA^3v^rr^2)=-P\left[\partial_t(UA^3)+\frac{1}{r^2}\partial_r(UA^3v^rr^2)\right] . \tag{17}$$

Momentum equation:

$$\partial_t(S_rA^3)+\frac{1}{r^2}\partial_r(S_rA^3v^rr^2)=-\alpha A^3\left\{\partial_rP+(D+E+PU)\times\left[U\partial_r\ln\alpha+\left[\frac{1}{U}-U\right]\partial_r\ln A\right]\right\}+S_rA^3\partial_r\beta . \tag{18}$$

The fluid velocity v^r and the generalized boost factor U are calculated from the normalization condition on the four-velocity.

The equations of motion of the field are obtained from $T^{(\text{field})}_{\mu\nu}$ in an exactly analogous manner; the calculations have been carried out by Park,[17] and the result is

$$\partial_t(A^3\varphi)+\frac{1}{r}\partial_r[r^2(-2\beta)A^3\varphi]=\alpha\frac{\pi}{r^2}-A^3\varphi(\beta\partial_r\ln\alpha+\alpha K) \tag{19}$$

and

$$\partial_t\pi=\partial_r\left\{\alpha A^3r^2\left[\frac{1}{A^2}-\frac{\beta^2}{\alpha^2}\right]\partial_r\varphi+A^3r^2\varphi\left[\partial_t\left[\frac{\beta}{\alpha}\right]-\beta K+\frac{2\beta^2}{\alpha r}+\frac{\beta}{\alpha}\partial_r\beta+\frac{3\beta^2}{\alpha}\partial_r\ln A\right]\right\}-\alpha A^3r^2V'(\varphi) , \tag{20}$$

where π, the conjugate momentum of the field, is defined by the equation

$$\partial_t\varphi=\frac{\alpha}{A^3r^2}\left[\pi+2\partial_r\left[\frac{\beta A^3r^2\varphi}{\alpha}\right]-\varphi\partial_r\left[\frac{\beta A^3r^2}{\alpha}\right]\right] . \tag{21}$$

A factor of $\sin\theta$ has been absorbed into the definition of π; this is natural for spherical symmetry, but in higher-dimensional three-geometries, the factor of A^3r^2 would be replaced by $A^3r^2\sin\theta$.

To complete the specification of the problem, we need only determine an equation of state for the pressure P. This pressure is due to the fluid only, and since the "fluid" is radiation in our case, the appropriate equation of state is

$$PU=\tfrac{1}{3}E . \tag{22}$$

Boundary conditions are specified by demanding that all variables must take the values appropriate to a radiation-dominated Einstein–de Sitter model. In isotropic coordinates, the Robertson-Walker metric takes the form

$$ds^2=-dt^2+\frac{R^2(t)}{1+\frac{1}{4}kr^2}(dr^2+r^2d\theta^2+r^2\sin^2\theta\, d\phi^2)\ , \tag{23}$$

from which we immediately obtain our "zeroth-order" boundary conditions for the metric quantities. We shall also require that, at the outer edge of the mesh,

$$\varphi_B=\sigma\ , \tag{24a}$$

$$\partial_r\varphi=0\ , \tag{24b}$$

$$\partial_t\varphi=0\ , \tag{24c}$$

and

$$\pi_B=0\ . \tag{24d}$$

D_B and E_B are obtained from the usual Friedmann-Robertson-Walker (FRW) relationships by the formulas

$$D_B^{n+1}=D_B^n\left[\frac{R^n}{R^{n+1}}\right]^3,\quad E_B^{n+1}=E_B^n\left[\frac{R^n}{R^{n+1}}\right]^4, \tag{25}$$

where n denotes the nth time step. $R(t)$ and its time derivatives are obtained from

$$\ddot{R}=-\frac{4\pi}{3}R[\rho+\rho\epsilon+3P+2(\partial_t\varphi)^2-2V(\varphi)] \tag{26a}$$

and

$$\dot{R}^2=\frac{8\pi}{3}R^2[\rho+\rho\epsilon+\tfrac{1}{2}(\partial_t\varphi)^2+V(\varphi)]\ . \tag{26b}$$

When $\partial_t\varphi$ and $V(\varphi)$ are zero, these obviously reduce to the familiar equations for a FRW spacetime. Since these conditions will hold in our case, and our background is the Einstein–de Sitter solution, we obtain, with an appropriate choice of the constants of integration, $R=t^{1/2}$. The code numerically integrates Eqs. (26) to find the value of the expansion parameter on a given time slice; checking its results against the known solution confirms that this computation is extremely accurate.

III. NUMERICAL CONSIDERATIONS

A. The code

The code used to solve Eqs. (10)–(14) and (16)–(20) is based on a general-purpose, spherically symmetric cosmology code.[18] To adapt the code to the inflationary cosmologies, all that was necessary was the insertion of the scalar-field terms in Eqs. (10)–(13), and the addition of the subroutines needed to evolve the scalar field and its conjugate momentum. Briefly, the code is an explicit, Eulerian code which solves the Einstein equations by means of finite-differencing algorithms; the differencing is carefully constructed to reduce or eliminate the problems due to the coordinate singularities that occur in curvilinear coordinates.[19] Equations (11) and (12) are simple quadratures and are solved by the trapezoid method. The hydrodynamic equations (16)–(18) are solved by means of a modern, highly accurate transport algorithm.[20] The scalar-field evolution equations are solved by methods similar to those used for the other equations; since Eq. (19) is in the form of a transport equation, it was treated by the same techniques employed for the hydrodynamical transport. The conjugate-momentum equation (20) was solved by a straightforward differencing technique. For both the scalar-field equation and the conjugate-momentum equation, it was found that stability was greatly enhanced by the use of a multistep method, in which the final solution on a time step is computed from a weighted sum of the new (nth) time level and the previous (n-1st) solution; the particular multistep technique employed is usually known as the second-order Adams-Bashforth algorithm.

Numerical cosmology is a young field, and many fundamental questions are not yet resolved; it is not even known what is the most appropriate choice for the time-slicing criterion. The behavior of the present code is indicative of marginal stability, but the cause of this problem is not well understood. In the case of the FRW solutions, precise cancellations occur in the sources of Eqs. (10) and (13); it is possible that such cancellations might suppress spurious exponential solutions which could lurk in this time slicing. For example, if we ignore the spatial term in Eq. (14), we note that the equation resembles that for a growing exponential (recall that $K<0$ in this slicing) regardless of the energy content of the Universe; only the specific time dependence of K prevents such a solution. In any event, we have found that we have been forced to use extremely small spatial and time steps, making the code quite expensive to run. When the code's limitations are respected, however, it is capable of producing very accurate results, as our code tests indicate.

Because of the numerical problems, a thorough exploration of parameter space was not possible. We selected values deemed reasonable and watched the evolution of the spacetime, but we were unable to carry out enough runs to classify the results based on parameter values. It is not clear that such a classification would be particularly meaningful, at any rate. As we shall explain later, the range of parameters thought to be "realistic" for the potential was beyond our capabilities; moreover, the form we chose for our initial scalar field was arbitrary and was meant only to indicate the behavior of an inhomogeneous field with a reasonably smooth amplitude function.

B. Code tests

The gravitational and hydrodynamical aspects of the code have already been tested.[21] For our current purposes, we have performed several tests of the scalar-field aspects of the code.

1. The homogeneous case

The obvious homogeneous test cases are the known solutions utilizing the Coleman-Weinberg potential for the scalar field. Two exact solutions will be considered: that for which $\varphi=\sigma$ everywhere, and that for which $\varphi=0$ identically. In both cases, the fluid content of the spacetime is pure radiation ($D=0$, $PU=\frac{1}{3}E$). For the homogeneous tests we shall start from initial conditions $t_0=1$, $E_0=3/32\pi$, and $R_0=1$.

First we treat the case $\varphi=\sigma$. This solution does not inflate. This test also confirms the ability of the code to maintain the background FRW values of the gravitational and fluid quantities, since they should be unaffected by the presence of the scalar field. Input parameters were chosen to be $\sigma=0.1$, $\lambda=0.01$, $V=0$, $\Delta r=0.1$, and $\Delta t=0.02\Delta r$.

The results of this test were excellent; after 50 000 time steps, the time had advanced from $t=1$ to $t=101$, an increase of more than a factor of 100, yet the error in the φ field was no more than a few parts in 10 000; specifically, it was correct to within 0.02%. The radiation energy density was accurate to 0.5%, while the metric variable was correct to within 3.5%, and the lapse to 0.02%. In this case, we were able to run the code with relatively large step sizes, with 100 zones covering the spatial grid. In light of the marginal stability of the code, these step sizes are quite generous; they are made possible by the fact that A does not change rapidly in either space or time.

Similar results were obtained for the case $\varphi=0$, although with a much more severely restricted spatial step size. This case inflates rapidly; it can be shown that the exact solution for the expansion factor is given by

$$R^2=\left[\frac{E_0R_0^4}{V_0}\right]^{1/2}\sinh\left[\left[\frac{32\pi V_0}{3}\right]^{1/2}t\right], \tag{27}$$

where E_0, R_0, and V_0 are, respectively, the initial values of the energy density, scale factor, and potential. This solution resembles that for an "ordinary" $k=-1$, radiation-dominated, FRW cosmology, which is not scale free. It is simplest, however, to set initial conditions for $t_0\ll 1$, in which case we can set t_0 arbitrarily and allow R_0 and E_0 to take their Einstein–de Sitter values of, respectively, $t_0^{1/2}$ and $3/32\pi R_0^4$. Unfortunately, under these circumstances a very small initial time results in a large difference in scale between the relatively small expansion parameter and the very large initial energy density; the code then has great difficulty in picking out the solution to the constraints, especially in an inflationary case. Nevertheless, the error resulting from the use of approximate initial values should not be serious even for larger t_0, provided it is not *too* large, so we used the same values for these initial parameters as for the previous homogeneous test case. The other parameters needed were given initial conditions as follows: $\sigma=1$, $\lambda=0.01$, $V_0=\lambda\sigma^4=0.005$, $\Delta r=0.01$, and $\Delta t=0.1\Delta r$.

We found at $t=31$, after 30 000 time steps, that

$$R_{\rm num}=626.0\ . \tag{28a}$$

This should be compared to the analytic value

$$R_{\rm an}=629.3\ . \tag{28b}$$

The value of A varied across the grid by approximately 0.06% (it should be strictly constant), while E is homogeneous to 0.05%. The value of E is correct to 0.2%, and the lapse is accurate to 0.03%. The shift and the extrinsic-curvature variable K^*, both of which should vanish identically in any FRW spacetime, are approximately 10^{-13} or smaller in magnitude, well below the level of the noise.

2. *The inhomogeneous case*

An inhomogeneous test solution can be obtained for the scalar field, if some simplifying assumptions are made. If we assume a free scalar field ($V=0$), and, further, assume that the scalar field does not act on the gravitational field (but the gravitational field does influence the scalar field), and then take the gravitational field to be given by a pure $k=0$, FRW, radiation solution, then we may obtain an analytic solution to Eqs. (19) and (20). This solution is, with suitable initial and boundary conditions,

$$\varphi(r,t)=j_0(2(t/t_0)^{1/2})j_0(R_0r/t_0) \tag{29}$$

and

$$\pi(r,t)=\tfrac{1}{2}R_0^2(t/t_0)^{1/2}r\sin(R_0r/t_0)\times\{\cos[2(t/t_0)^{1/2}]-j_0(2(t/t_0)^{1/2})\}\ , \tag{30}$$

where j_0 is the spherical Bessel function of order zero. Note that we solve for π/r^2 rather than for π itself; the latter never appears explicitly, and evolving π/r^2 helps to minimize problems at the origin.

For our run, the initial conditions were set up with $t_0=100$ and $R_0=10$, and the evolution was carried out for 36 000 cycles, to $t=7300$. In this case, $\Delta r=2$ and we used 500 zones. The results are displayed in Fig. 1. Figure 1(a) is a plot of the scalar field, while Fig. 1(b) shows the conjugate momentum π/r^2. Agreement is excellent for the scalar field itself; on the scale of the plot, the analytic and numerical curves are indistinguishable. The ability of the code to follow the field's oscillations so well for so many time steps is particularly striking. The conjugate momentum shows a much larger error. Obviously, the error in the conjugate momentum is largest near the origin. We have applied all the regularization techniques employed in other parts of the code, as well as absorbed a factor of $1/r^2$ into the definition of π; these techniques drastically reduced the coordinate error, but did not eliminate it. Further work is necessary to find the appropriate regularization technique(s) for this equation. Fortunately, this error propagates into the scalar field only very slowly, and since the other variables (in particular, the gravitational variables) see only φ, they should be relatively unaffected by this problem.

It is difficult to cite a relative error in this case because of the tendency of a numerically evolved wave to develop a phase error with respect to the analytic solution. A zone-by-zone comparison is thus misleading and tends to overestimate the error in the amplitude. However, this type of error is small near the origin; there the relative error in φ is less than 2.5%, whereas the relative error in π is approximately 18%. It is obvious from the plots in Fig. 1 that these figures represent upper bounds for the relative error on this time step.

It should be pointed out in connection with these test

cases that the critical parameters in determining stability for a code of this nature are not the absolute values of Δr and Δt, but rather the ratios $\Delta t/\Delta r$ and $\Delta r/r_{\max}$. For the test cases, we have found that we must restrict these ratios roughly as

$$\frac{\Delta t}{\Delta r} \lesssim 0.02 \tag{31a}$$

and

$$\frac{\Delta r}{r_{\max}} \lesssim 0.01 \ . \tag{31b}$$

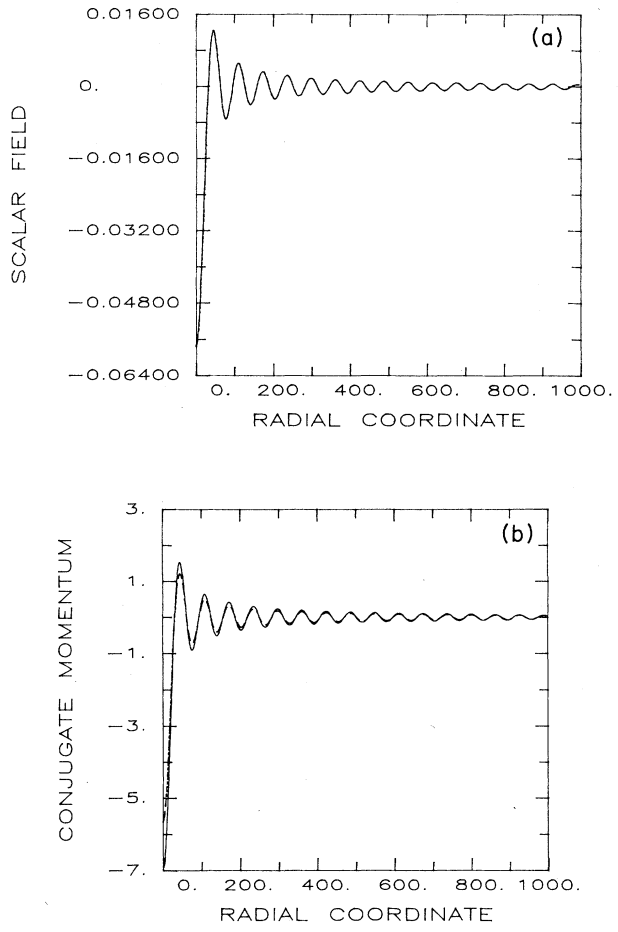

FIG. 1. Inhomogeneous-field test case. The background is assumed to be a pure Einstein–de Sitter spacetime, which is unaffected by the presence of the scalar field, although the field is influenced by the background. For this run, we used 500 zones, with $\Delta r=2$. We started from an initial time $t=100$; the results are displayed at $t=7300$, after 36 000 cycles. The solid curve is the analytic solution, given by Eqs. (29) and (30), while the dashed curve is the numerical result. (a) The scalar field. The relative error is less than 2.5%; phase error is virtually nonexistent despite the large number of wavelengths contained within the grid. (b) The corresponding conjugate momentum. An error near the origin leads to a large (approximately 18%) relative error there, but farther out, the results are excellent.

For our circumstances, the appropriate speed for the Courant-Friedrichs-Lewy (CFL) criterion is the speed of light; since we take that to be unity, the CFL condition alone requires that $\Delta t < \Delta r$. Clearly, (31a) is far more restrictive than this. The very small time step, as well as the small spatial step size, was necessary in order to keep the *gravitational* solvers stable; the scalar field alone could be evolved with a much larger time step. As long as these limitations are respected, however, we can scale our mesh to whatever values are appropriate for our problem.

IV. RESULTS

Our purpose was to determine whether an inhomogeneous scalar field, the form of which met certain criteria but was otherwise arbitrary, would cause the spacetime to evolve to form a "child" universe. We took as our ansatz for the field that initially

$$\varphi_0=\sigma\{1-c_0\exp[-(r/c_1)^2]\} \ , \tag{32a}$$

$$\pi_0=\partial_t\varphi=0 \ , \tag{32b}$$

where c_0 and c_1 are constants. This form has the property that, for reasonable values of the parameters, it goes to a constant at the boundary sufficiently rapidly to satisfy the demands of the code. It approaches the false vacuum near the origin and the true vacuum near the outer boundary, and it makes a smooth transition between the two; since we have no knowledge of the actual shape the scalar field might take in the early Universe, this form is as reasonable as any.

We must also make a choice for the initial energy density of the radiation. For a spacetime containing a scalar field on a strictly Einstein–de Sitter background, the total energy density, including that due to the scalar field, is

$$E=\frac{3}{32\pi t^2}+\{\tfrac{1}{2}[(\partial_t\varphi)^2+(\partial_r\varphi/R)^2]+V(\varphi)\} \ , \tag{33}$$

where

$$E_{\rm rad}=\frac{3}{32\pi t^2} \tag{34}$$

is the energy density due to the radiation energy density alone. Because of the expense of running the code, however, we must choose a spacetime that is initially sufficiently inhomogeneous that we can hope to see the effect in a feasible running time. For the cases attempted, initializing the total energy density based on (32) and (33) resulted in the failure of the Hamiltonian-constraint solver to converge. Some of the initial inhomogeneity must be carried by the radiation energy density. It was found that when we set the radiation energy density to be

$$E_{\rm rad}=\frac{3}{32\pi t_0^2}-\tfrac{1}{2}(\partial_r\varphi)^2-V(\varphi) \ , \tag{35}$$

we were able to obtain successful runs. The form of (35) was chosen in order to "flatten" the total initial energy density so as to ensure convergence of the Hamiltonian constraint, while still allowing inhomogeneous initial conditions. This expression also approaches the Einstein–de Sitter solution at the outer boundary, as it

must to meet the boundary-condition requirements of the code.

The parameters of the CW potential were set to the following values:

$$\sigma = 0.1 \ , \tag{36a}$$

$$\lambda = 0.01 \ . \tag{36b}$$

These values are not entirely consistent with current beliefs about the magnitude of the potential in the early Universe; arguments based on the theory of galaxy formation indicate that the limits on these parameters should be $\sigma_{\rm gf} \approx 1$, $\lambda_{\rm gf} \approx 10^{-17}$, and $t_{0({\rm gf})} \approx 10^{8}$. Unfortunately, our code was unable to perform runs with these values. For such input parameters, the potential is $V_{\rm gf} \approx 5 \times 10^{-18}$ near the origin, while $A \approx 10^{4}$. This difference in scale was simply too great for the code to handle; the Hamiltonian constraint solver was unable to converge to the correct initial data. This is disappointing but not too surprising; the plane-symmetric code used by Kurki-Suonio, Centrella, Matzner, and Wilson[22] was also unable to deal with such values of the parameters.[23]

In all our "production" runs, we used

$$\Delta r = 1 \ , \tag{37a}$$

$$r_{\rm max} = 1000 \ (1000 \text{ zones}) \ , \tag{37b}$$

$$t_0 = 100 \ , \tag{37c}$$

$$R_0 = 10 \ ,$$

$$\Delta t = 0.02 \Delta r \ . \tag{37d}$$

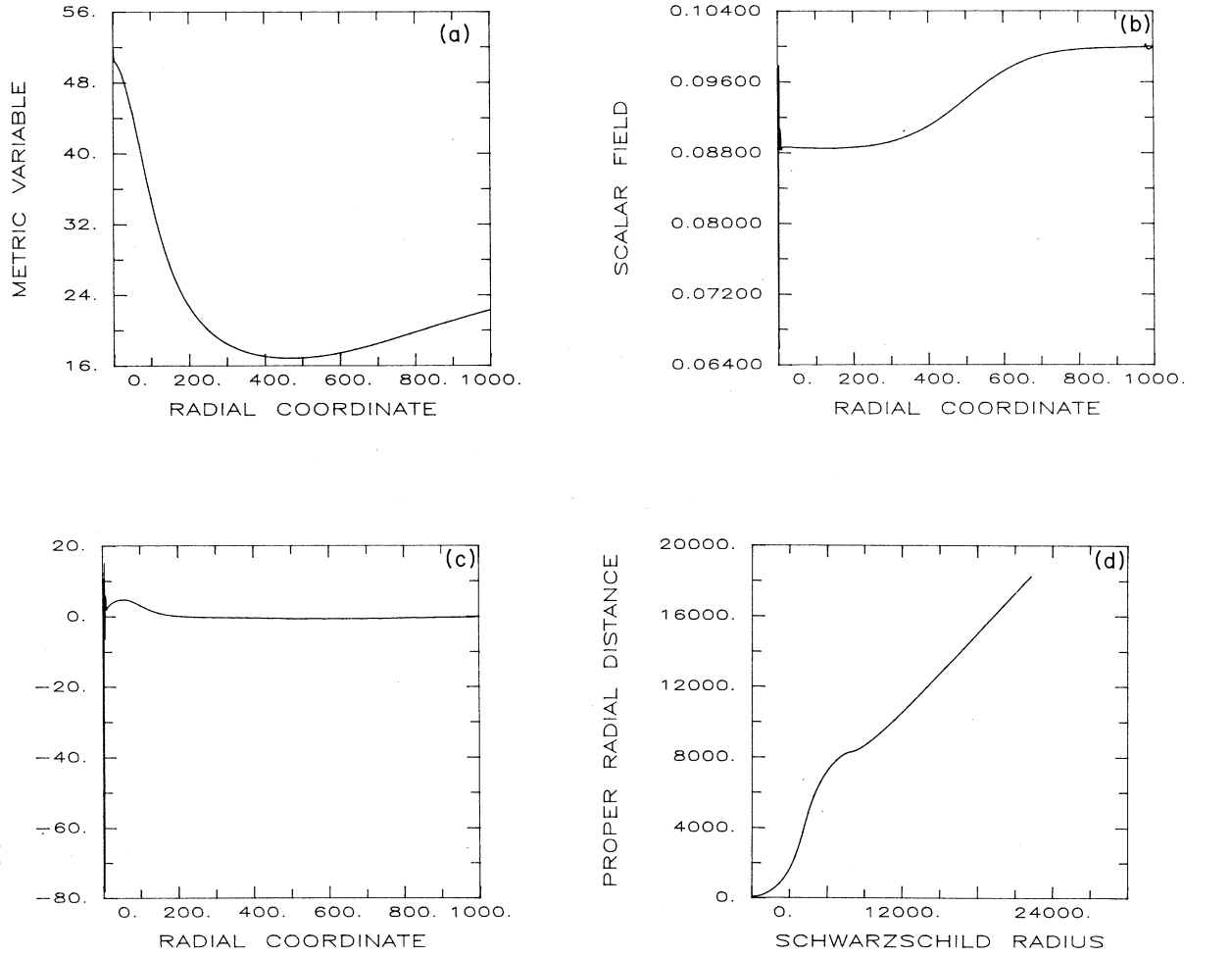

FIG. 2. The results of a run which did not form a "child" universe. In this case we used 1000 zones, with $\Delta r = 1$. Initially $\varphi = \sigma\{1 - 0.9 \exp[(r/500)^2]\}$. Results are shown for $t = 500$. (a) The metric variable. The error near the origin is beginning to propagate into this variable, but its effect is still quite small. (b) The scalar field. The spike near the origin is a numerical error, but may result from domain-wall formation, which our code cannot resolve. The small error evident near the outer boundary is probably due to the imposition of "zeroth-order" boundary conditions at the edge of a finite mesh. (c) The conjugate momentum. (d) The proper radial distance, defined such that the distance along the curve is the proper arc length, versus the Schwarzschild radius $Ar_{\rm isotropic}$.

For all cases we chose for the field parameters [cf. Eq. (32a)]

$$c_1 = 500 , \tag{38}$$

while c_0 varied.

In all cases studied, we found that the scalar field tended to quickly develop a rapid change, almost a discontinuity, near the origin, as shown in Figs. 2(b) and 3(b). While the "spike" itself is clearly a numerical artifact, we consider it likely that it may have a physical instigator, such as the formation of a domain wall between the region of false vacuum and true vacuum; this behavior would be consistent with that observed by Kurki-Suonio, Centrella, Matzner, and Wilson.[24] The possibility merits investigation; unfortunately, the present code is inadequate for such a task. In order for the details of the formation of a wall to be clarified, a new code would have to be developed whose purpose was specifically the study of this process; it would probably be necessary to develop a technique analogous to the artificial viscosity of classical numerical hydrodynamics, and/or an adaptive-mesh approach which could rezone the mesh in regions of large gradients, for the equations which evolve the scalar field and the conjugate momentum.

We found that the global behavior of the spacetime was different for different values of c_0. For $c_0 = 0.9$, we were unable to see any "pinching" behavior. The results of this run are displayed in Fig. 2 at $t = 500$, after 20 000 cycles. It is obvious that we are at or beyond the limit of our resolution for the scalar field, yet, as Fig. 2(d) shows, no throat has formed; it is unclear whether the wormhole would have formed had we been able to extend the run further, but it appears that inflation is faltering by the time the run was terminated. Similar results were obtained for those cases studied with $c_0 < 0.9$.

The situation was quite different for $c_0 = 0.95$, the results of which are displayed in Fig. 3. The plots show the evolution at 12 000 cycles, corresponding to $t = 340$; the

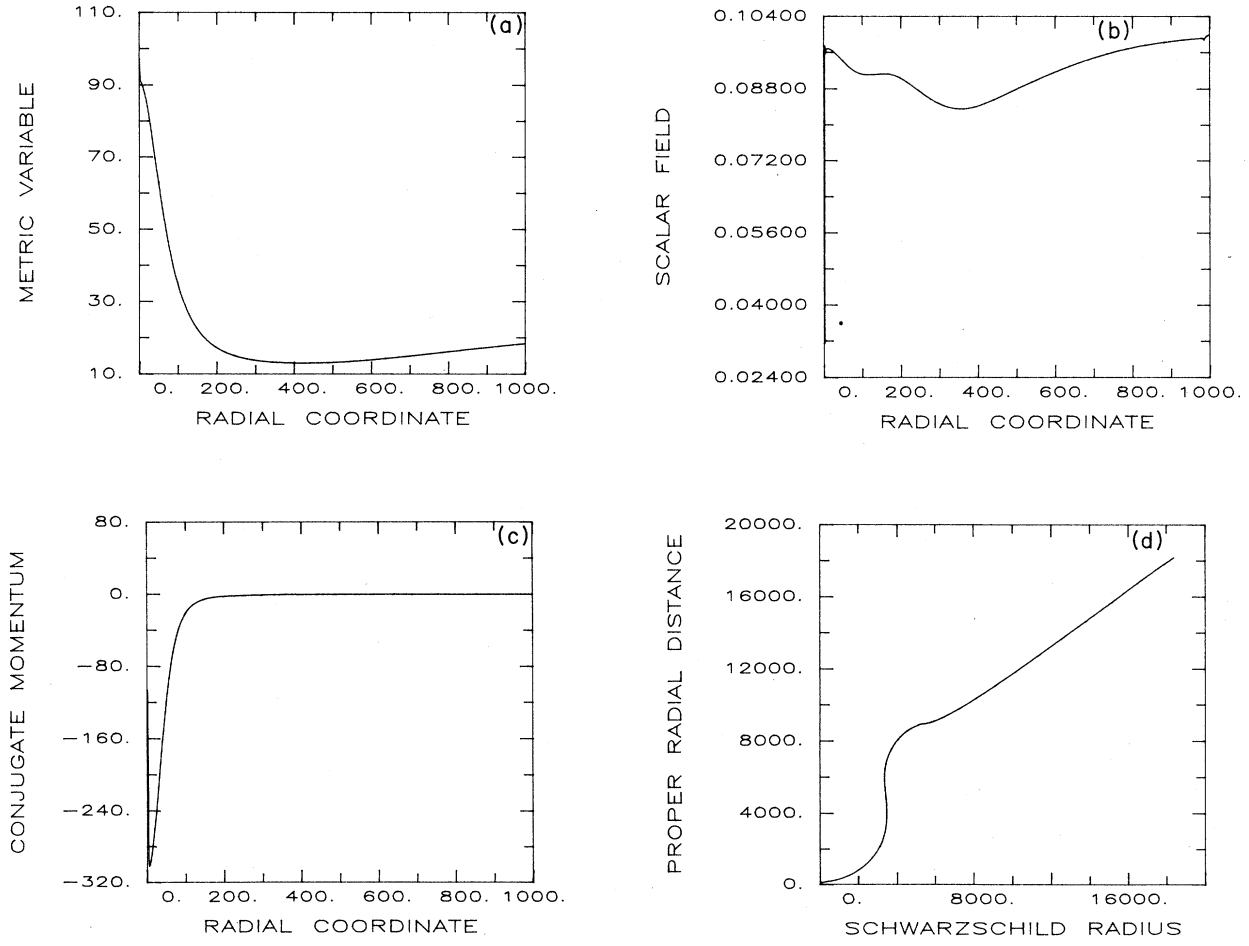

FIG. 3. A run in which a throat did form. In this case, the initial scalar field was given by $\varphi = \sigma\{1 - 0.95\exp[(r/500)^2]\}$. Once again, 1000 zones were used. These plots represent the results at $t = 340$. (a) The error near the origin is noticeable in this case also, but is still small. (b) Like Fig. 2(b). (c) Like Fig. 2(c). (d) Like Fig. 2(d), but here we see the initial stage of the formation of the "child" universe.

run continued well beyond this, but by this point we are losing the ability to resolve the scalar field. (It should be noted, however, that there are 100 zones between the origin and the first minor tick mark, so we still have some resolution of the scalar field quantities there.) Already a throat appears to be well on its way in forming. Even with good resolution of φ, we would probably not be able to follow the development of the wormhole much farther than this, however, because of a problem with patching; as York has pointed out,[25] an inconsistency will develop in the slicing before the throat is fully formed. This occurs because the appropriate slicing for the external universe is the constant-mean-curvature criterion, but near the throat we should use maximal ($K=0$) slicing. This conjecture deserves further investigation if more detailed studies of the behavior of an inhomogeneous scalar field are to be carried out.

V. CONCLUSIONS

We have computed the first stages of the formation of a "child" universe in a spherically symmetric, $k=0$ cosmology which contains a nonidealized inhomogeneous scalar field, thus demonstrating that such a phenomenon might occur under quite general conditions in an inflationary universe. It should be pointed out that no particular "fine-tuning" of the parameters was required to obtain the effect; the only restrictions placed on their values were those resulting from numerical considerations. The problem warrants more realistic simulations, which would require the development of a new code. The current code is not sufficiently robust to follow the evolution for long periods, nor is it able to follow the details of the interface between the true vacuum and the false vacuum. Moreover, there are theoretical problems associated not just with the scalar-field aspects of the code, such as the patching problem discussed above, but also with numerical cosmology in general, which must be addressed before substantial further progress can be made. When these issues are resolved, however, the study of the evolution of inhomogeneous cosmologies could add much to our understanding of the early Universe.

ACKNOWLEDGMENTS

We wish to thank A. Guth, H. Kurki-Suonio, and J. York for helpful discussions. This work was partially supported by NSF Grant No. AST-8644602. E.T.V. thanks the Alfred P. Sloan Foundation for support. Computing resources were provided by the Computation Center of the University of Texas at Austin and the University of Texas System Center for High Performance Computing.

[1]A. H. Guth, Phys. Rev. D **23**, 347 (1981).
[2]A. D. Linde, Phys. Lett. **108B**, 389 (1982).
[3]A. D. Albrecht and P. J. Steinhardt, Phys. Rev. Lett. **48**, 1220 (1982).
[4]A. D. Linde, in *Three Hundred Years of Gravitation,* edited by S. W. Hawking and W. Israel (Cambridge University Press, Cambridge, England, 1987).
[5]K. Sato, H. Kodama, M. Sasaki, and K. Maeda, Phys. Lett. **108B**, 103 (1982).
[6]H. Kodama, M. Sasaki, K. Sato, and K. Maeda, Prog. Theor. Phys. **66**, 2052 (1981); H. Kodama, M. Sasaki, and K. Sato, *ibid.*, **68**, 1979 (1982); V. A. Berezin, V. A. Kuzmin, and I. I. Tkachev, Phys. Lett. **120B**, 91 (1983); S. K. Blau, E. I. Guendelman, and A. H. Guth, Phys. Rev. D **35**, 1747 (1987).
[7]S. K. Blau and A. H. Guth, in *Three Hundred Years of Gravitation* (Ref. 4).
[8]H. Kurki-Suonio, J. Centrella, R. A. Matzner, and J. R. Wilson, Phys. Rev. D **35**, 435 (1987).
[9]R. Arnowitt, S. Deser, and C. W. Misner, in *Gravitation: An Introduction to Current Research,* edited by L. Witten (Wiley, New York, 1962).
[10]L. L. Smarr and J. W. York, Jr., Phys. Rev. D **17**, 2529 (1978).
[11]J. R. Wilson, in *Sources of Gravitational Radiation,* edited by L. Smarr (Cambridge University Press, Cambridge, England, 1979).
[12]C. W. Misner, K. S. Thorne, and J. A. Wheeler, *Gravitation* (Freeman, San Francisco, 1973).
[13]S. Coleman and E. Weinberg, Phys. Rev. D **7**, 1880 (1973).
[14]J. W. York, Jr., in *Sources of Gravitational Radiation* (Ref. 11).
[15]K. A. Holcomb, report, 1988 (unpublished)
[16]L. L. Smarr, C. Taubes, and J. R. Wilson, in *Essays in General Relativity,* edited by F. Tipler (Academic, New York, 1980).
[17]S. J. Park, Department of Astronomy, University of Texas at Austin report, 1986 (unpublished).
[18]Holcomb (Ref. 15).
[19]C. R. Evans, in *Dynamical Spacetimes and Numerical Relativity,* edited by J. Centrella (Cambridge University Press, Cambridge, England, 1986).
[20]See, for example, J. F. Hawley, L. L. Smarr, and J. R. Wilson, Astrophys. J. Suppl. **55**, 211 (1984). Our code uses the Barton method of numerical transport.
[21]Holcomb (Ref. 15).
[22]Kurki-Suonio *et al.* (Ref. 8).
[23]H. Kurki-Suonio (private communication).
[24]Kurki-Suonio *et al.* (Ref. 8).
[25]J. W. York, Jr. (private communication).